

The Research Scanning Polarimeter: Calibration and Ground-based Measurements

Brian Cairns^a, Edgar E. Russell^b and Larry D. Travis^c

^aDepartment of Applied Physics and Applied Mathematics, Columbia University, New York

^bSpecTIR Corporation, Santa Barbara, CA.

^cNASA Goddard Institute for Space Studies, New York

ABSTRACT

SpecTIR Corporation has recently completed building the Research Scanning Polarimeter (RSP). This instrument was designed to provide highly accurate polarimetric measurements both from aircraft and from the ground. The spectral range of the measurements is from 410nm to 2250nm and the field of view of the instrument is scanned over a 120° swath ($\pm 60^\circ$ from nadir/zenith). Here we describe the results of the instrumental calibration and the quantitative interpretation of ground-based measurements. Recently we have acquired data using the RSP on an aircraft and a brief discussion of the information content of this data and some preliminary aerosol retrievals over the Pacific ocean are presented.

1. INSTRUMENT DESCRIPTION

The RSP instrument uses a polarization compensated scan mirror assembly to scan the fields of view of six boresighted, refractive telescopes through $\pm 60^\circ$ from the normal with respect to the instrument baseplate. The refractive telescopes are paired, with each pair making measurements in three spectral bands. One telescope in each pair makes simultaneous measurements of the linear polarization components of the intensity in orthogonal planes at 0° and 90° to the meridional plane of the instrument, while the other telescope simultaneously measures equivalent intensities in orthogonal planes at 45° and 135° . This approach ensures that the polarization signal is not contaminated by scene intensity variations during the course of the polarization measurements, which could create false polarization. These measurements in each instantaneous field of view in a scan provide the simultaneous determination of the intensity, and the degree and azimuth of linear polarization in all nine spectral bands.

The instrument has nine spectral channels that are divided into two groups based on the type of detector used: visible/near infrared (VNIR) bands at 410 (30), 470 (20), 550 (20), 670 (20), 865 (20) and 960 (20) nm and shortwave infrared (SWIR) bands at 1590 (60), 1880 (90), and 2250 (120) nm. The parenthetical figures are the full width at half maximum (FWHM) bandwidths of the spectral bands. These spectral bands sample the spectrum of reflected solar radiation over most of the radiatively significant range, with measurements under typical clear sky conditions ranging from significant Rayleigh scattering (410nm) to single scattering by aerosol (2250nm) within a single measurement set.

The desired polarization-insensitive scanning function of the RSP is achieved by the use of a two-mirror system with the mirrors oriented such that any polarization introduced at the first reflection is compensated for by the second reflection. Boresighted refractive telescopes define the 14mrad field of view of the RSP. Dichroic beam splitters are used for spectral selection, interference filters define the spectral bandpasses and Wollaston prisms spatially separate the orthogonal polarizations onto the pairs of detectors. The detectors for the VNIR wavelengths are pairs of UV-enhanced silicon photodiodes. The detectors for the SWIR wavelengths are pairs of HgCdTe photodiodes with a 2.5 μm cutoff cooled to 163K.

With the exception of the dual preamplifiers located near each detector pair, the RSP electronics is contained within three stacked, interconnected modules. The electronics provides the amplification of the signals detected by the 36 detector channels, sampling and 14-bit analog-to-digital conversion of the resultant signals, the servo control of the scanner rotation and temperature of the SWIR detectors, and the control logic that formats the instrument signal and housekeeping data and supports transmission of the digital data to a personal computer for storage. A liquid nitrogen dewar is used to cool the SWIR detectors during both ground and airborne operation. To optimize the performance of the SWIR channels the temperature of the detectors is servo controlled at 163K during operation. Digital data from 152 scene sectors (IFOVs) over 121 degrees of scan, dark samples from 10 sectors and instrument status data are formatted by the RSP electronics and transmitted each scan to a personal computer for storage. The average data rate of 110kbps provides readout of the 36 signal channels together with instrument status data at a scan rate of 71.3 rpm. This scan rate results in an IFOV dwell time of

1.875 msec and yields contiguous (scan line-to-line) coverage at nadir for an aircraft travelling at a V/H ratio of 0.017sec^{-1} , e.g., 100 knots at an altitude of 3048m (10,000 ft.). The instrument mass is 24kg (including LN2), its size is 48 x 28 x 34 cm (Length x Width x Height) including dewar, and the power required for the instrument itself is 18W (27W peak).

2. CALIBRATION

We denote the set of four measurements in a particular band to be S1L and S1R for the two orthogonal polarization states in telescope 1 and S2L and S2R for the two orthogonal polarizations in telescope 2. Since the gains of the detectors in all the telescopes are not identical the first three Stokes parameters are related to the four measurements by the following expressions

$$\begin{aligned} I &= \frac{(S1L + K1.S1R)}{A} = \frac{C12(S2L + K2.S2R)}{A} \\ Q &= \frac{(S1L - K1.S1R)}{A} \\ U &= \frac{C12(S2L - K2.S2R)}{A}. \end{aligned} \quad (1)$$

The meaning of the different relative calibration coefficients is clear. K1 is the ratio of the gains of the detectors measuring S1L and S1R, while K2 is the ratio of the gains of the detectors measuring S2L and S2R. For the polarimetric calibration of the instrument, which is discussed in section 2.1, we are interested in evaluating the coefficients K1 and K2 and any instrumental polarization effects. C12 is the ratio of the gain of the detectors in telescope 1 to the gain of the detectors in telescope 2 and is the easiest calibration coefficient to determine. This is because it can be estimated from *in situ* field measurements, or measurements viewing a reflectance standard since the 1 and 2 telescopes are boresighted and observe the same field of view. We use a Spectralon reflectance standard, made from a pure sintered polytetrafluorethylene (PTFE) material, that is made by Labsphere Inc. Thus C12 is simply the ratio of intensities measured using the two different telescopes, i.e.,

$$C12 = \frac{(S1L + K1.S1R)}{(S2L + K2.S2R)}.$$

Typically the dispersion in estimating C12 from the measured intensities during a few minutes of data acquisition (around 10,000 data points) is of the order 0.01% and is really an indication of how good the boresighting of the different telescopes and the signal to noise ratio is. The real limit on knowledge of C12 is stability. Although C12 is stable at the 1% level over a period of 6 months slow drifts at this level can occur during the course of a day, or between days. This indicates that to obtain the most accurate value of this factor the estimate should be updated quite frequently (hourly), using *in situ* data. The radiometric calibration of the instrument defines the coefficient A and will be discussed in section 2.2.

2.1 Polarimetric Calibration

In evaluating the polarimetric calibration of the RSP we will be interested in the normalized values of the Stokes parameters Q and U, viz., $q(=Q/I)$ and $u(=U/I)$, since these quantities are independent of the radiometric calibration, or knowledge of C12. The instrument's polarimetric performance has been examined using sources that provide unpolarized light, weakly polarized light and completely polarized light.

The unpolarized light is provided by viewing a Spectralon reflectance standard through a polarization scrambler. The polarization scrambler is designed to randomize the orientation of polarization of incident polarized light so that the net effect is to provide transmitted light with negligible average polarization. The efficiency of the polarization scrambler can be tested by making measurements with the RSP that allow the scene polarization to be accurately determined, independent of instrumental polarization effects, or knowledge of K1 and K2. Consider a set of measurements of the same scene with the RSP instrument rotated to 0° and 90° about its line of sight. Using the definition

$$\eta(\theta) = \frac{S1L(\theta)}{S1R(\theta)} \quad r_2(\theta) = \frac{S2L(\theta)}{S2R(\theta)},$$

then for a weakly polarized scene we have the following simple model for the set of three measurements viz.,

$$\begin{aligned}\frac{\eta(0) - K1}{\eta(0) + K1} &= q_{inst} + q_{scene} & \frac{r_2(0) - K2}{r_2(0) + K2} &= u_{inst} + u_{scene} \\ \frac{\eta(90) - K1}{\eta(90) + K1} &= q_{inst} - q_{scene} & \frac{r_2(90) - K2}{r_2(90) + K2} &= u_{inst} - u_{scene}\end{aligned}$$

where q_{inst} and u_{inst} represent instrumental polarization effects while q_{scene} and u_{scene} are the relative q and u values of the scene observed by the instrument. The measurements at 0° and 90° are related to the instrumental and scene polarization by the following expressions

$$\frac{1}{2} \frac{\eta(0) - \eta(90)}{\eta(0) + \eta(90)} = \frac{q_{scene}}{1 + (q_{scene}^2 - q_{inst}^2)} \quad \frac{1}{2} \frac{r_2(0) - r_2(90)}{r_2(0) + r_2(90)} = \frac{u_{scene}}{1 + (u_{scene}^2 - u_{inst}^2)}$$

If the scene and instrumental polarization are small (less than 1%) then the quadratic terms are negligible and we can estimate the scene polarization from the formulae

$$q_{scene} \approx \frac{1}{2} \frac{\eta(0) - \eta(90)}{\eta(0) + \eta(90)} \quad u_{scene} \approx \frac{1}{2} \frac{r_2(0) - r_2(90)}{r_2(0) + r_2(90)} \quad (2)$$

It should be noted that given the form of the exact expression for scene polarization, neglecting instrumental polarization means that we will tend to overestimate the scene polarization. The scene polarization, q and u , derived using formula (2) is given in the following table. Column A is solar illuminated Spectralon viewed through the polarization scrambler for data on 10-08-98, column B is tungsten lamp illuminated Spectralon viewed through the polarization scrambler for data on 10-30-98 and column C is solar illuminated Spectralon from 10-08-98. The band 8 detectors in telescope 1 are not working so there is no estimate of q for this band. The estimate of u in band 8 is given only for the tungsten lamp illumination, column B, because of strong atmospheric absorption in this band leading to very low solar illumination levels. q and u values are not given for tungsten illumination for bands 1, 2 and 3 because of low signal levels in these bands for tungsten illumination. Column C indicates how much stronger the polarization signal is from Spectralon compared with Spectralon viewed through a polarization scrambler i.e., this illustrates that viewing Spectralon alone does not provide an acceptable source if completely unpolarized light is required. Columns A and B show that by viewing the Spectralon through a polarization scrambler the scene polarization can be reduced to less than 0.1% in all bands and is generally substantially less than this. The same results were found with four other similar sets of data taken on other days and, as noted above, the values of scene polarization values given here are if anything overestimates of the true scene polarization.

	A		B		C	
Band	q(%)	u(%)	q(%)	u (%)	q (%)	u (%)
1	0.014	0.007			1.628	0.250
2	-0.012	-0.010			1.762	0.388
3	0.013	0.014			1.716	0.471
4	-0.001	0.003	-0.076	0.044	2.058	0.534
5	0.017	-0.010	0.044	0.007	2.042	0.590
6	0.033	-0.029	-0.040	-0.021	2.303	0.583
7	0.065	0.077	0.049	0.023	2.601	0.738
8				-0.065		
9	0.073	-0.079	0.010	0.018	3.475	0.846

Table I: Estimation of scene polarization for Spectralon (C) and Spectralon viewed through a polarization scrambler (A & B).

We will now examine how well the values of K1 and K2 can be estimated in the presence of instrumental polarization. When the RSP measures light reflected off a Spectralon target and transmitted through the polarization scrambler we have the situation that,

$$\frac{\eta(scrambler) - K1}{\eta(scrambler) + K1} = q_{inst} \quad \frac{r_2(scrambler) - K2}{r_2(scrambler) + K2} = u_{inst}$$

since the scene polarization, as shown in the table above, is negligible for the polarization scrambler. We now examine what the consequences are of neglecting the instrumental polarization and estimating the K values from the expressions

$$\hat{K}1 = \eta(\text{scrambler}) \quad \hat{K}2 = r_2(\text{scrambler})$$

These estimates are not the true values of the relative gain coefficients if there is actually any instrumental polarization, but are plausible estimators that we will examine to determine whether they provide acceptable estimates of the true scene polarization. If we measure a polarized scene, we have the following model for this measurement

$$\frac{\eta(\text{scene}) - K1}{\eta(\text{scene}) + K1} = q_T \quad \frac{r_2(\text{scene}) - K2}{r_2(\text{scene}) + K2} = u_T$$

where q_T and u_T include the effects of both scene and instrumental polarization. If we use the estimated K values from above we obtain the following equations for the estimated q and u values

$$\hat{q} = \frac{\eta(\text{scene}) - \hat{K}1}{\eta(\text{scene}) + \hat{K}1} \quad \hat{u} = \frac{r_2(\text{scene}) - \hat{K}2}{r_2(\text{scene}) + \hat{K}2}$$

We now need to determine how these estimates of q and u relate to the actual scene polarization. From the foregoing we can derive the following expressions

$$\hat{q} \approx q_{\text{scene}} - u_{\text{inst}} u_{\text{scene}} q_{\text{scene}} \quad \hat{u} \approx u_{\text{scene}} - q_{\text{inst}} u_{\text{scene}} q_{\text{scene}} \quad (3)$$

that are accurate to first order in the instrumental polarization. These expressions indicate that for weakly polarized scenes any instrumental polarization is compensated for by the method used to estimate the values of K1 and K2. Corrections for the effects of instrumental polarization on strongly polarized scenes can be made using (3), if necessary. Table II below shows the K1 and K2 estimates obtained from simply viewing Spectralon through a polarization scrambler and using the ratio of intensities. The stability of the K values shows that this estimate does not represent a limiting factor on the polarimetric accuracy of the instrument during the course of an experiment. Indeed the K values are extremely stable (0.1%) over a period of several months.

Band	K1					K2				
	'009'	'035'	'038'	'066'	'078'	'009'	'035'	'038'	'066'	'078'
1	0.97078	0.97083	0.97089	0.97113	0.97142	1.00623	1.00659	1.00682	1.00672	1.00625
2	1.00820	1.00853	1.00852	1.00862	1.00842	1.06062	1.06056	1.06062	1.06048	1.06033
3	0.98962	0.98961	0.98991	0.98992	0.98973	1.05584	1.05586	1.05600	1.05597	1.05620
4	1.06096	1.06111	1.06117	1.06125	1.06136	1.04909	1.04901	1.04894	1.04903	1.04884
5	0.95402	0.95408	0.95425	0.95442	0.95419	1.02327	1.02333	1.02333	1.02337	1.02352
6	1.04884	1.04857	1.04832	1.04839	1.04822	1.07894	1.07861	1.07879	1.07823	1.07733
7	0.96285	0.96549	0.96729	0.96761	0.96217	1.03661	1.03660	1.03648	1.03677	1.03656
8										
9	1.03690	1.03653	1.03558	1.03602	1.03418	1.06697	1.06712	1.06704	1.06706	1.06694

Table II: K values determined by viewing solar illuminated Spectralon through a polarization scrambler on 2-22-99. Scan sectors used were chosen by visual inspection of scans to be at the center of polarization scrambler.

The fact that instrumental polarization has the particular form of interaction with the scene polarization shown in (3) above can be used with measurements of scenes that have a known level of polarization to bound the level of instrumental polarization. Obviously the best type of polarized scene to use in evaluating the level of instrumental polarization from (3) is one that is completely polarized. To create scenes that were completely polarized we used pairs of polarizers that were mounted in series, with their polarization axes parallel to one another. HN22 polarizers were used to assess the 410, 470, 555 and 670nm bands while HR polarizers were used to assess the 865, 960, 1590, 1880 and 2250nm bands. For an ideal polarizer oriented at an angle χ with respect to the meridional plane of the instrument $q = \cos(2\chi)$ and $u = \sin(2\chi)$. However, we found that the sheet polarizers that we were using exhibited significant variations in the orientation of the polarizer zones across the polarizer sheet. If this is the case then the observed values of q and u will be

$$q = \cos[2\chi + \epsilon_f(x, y)] \quad u = \sin[2\chi + \epsilon_f(x, y)].$$

where $\mathcal{E}(x,y)$ represents the variation of polarizer zone orientation as a function of the physical location on the sheet that is being observed. This means that if we rotate the polarizer and look at the variation of q and u as a function of angle the variation in physical orientation of the polarizer zones will frequency modulate the observed signal. As long as the zones are relatively uniform ($\epsilon \ll 1$) the expressions given above can be simplified to

$$q = \cos(2\chi) - \mathcal{E}(x,y)\sin(2\chi) \quad u = \sin(2\chi) + \mathcal{E}(x,y)\cos(2\chi).$$

A simple demonstration of the non-uniformity of the polarizer zones is given in figure 1 for a HN22 polarizer.

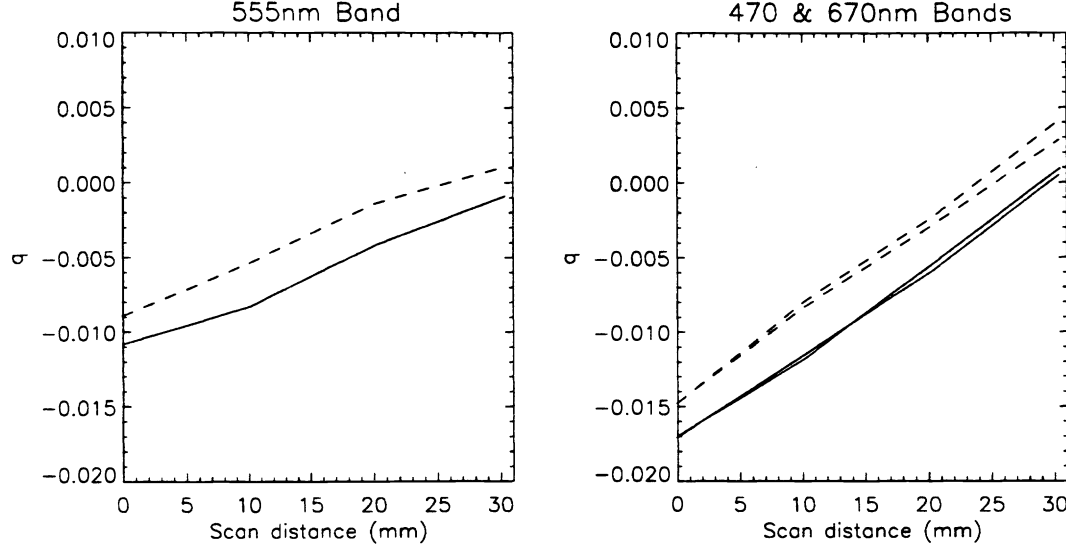


Figure 1: Raster scan of HN22 polarizer oriented at 45.5° to instrument meridional plane.

This figure shows a set of measurements that were taken for a fixed value of $\chi=45.5^\circ$ but with the physical location of the polarizer being moved in a raster scan. For this polarizer orientation $q = \mathcal{E}(x,y)$ so the measured values of q shown in the figure indicate the magnitude and spatial variation of the non-uniformity in the polarizer zones. The solid lines show measurements for one horizontal transect, while the dashed lines show measurements for a horizontal transect that is offset vertically by 10 mm from the first. The 470nm and 670nm bands are in the same telescope and should therefore see the same non-uniformities in the polarizer. This is seen in the right hand figure where the two solid lines and two dashed lines, that are the measurements for the different bands, are very close together. Similar results were found for the HR polarizers though the magnitude of the variation was only half as large as that found for the HN22 polarizers.

To try and circumvent this imperfection in the polarizers, we performed experiments where the polarizers were rotated through 360° with measurements being made every 15° . A Fourier analysis was then used to separate those terms that could only be caused by polarizer imperfections and those terms that can be caused by instrumental polarization. The deviation of the zones from their average orientation can be expressed as a Fourier expansion in the polarizer orientation

$$\mathcal{E}(x,y) = \sum_{n=1}^{\infty} a_n \cos(n\chi) + b_n \sin(n\chi)$$

where the coefficients in this expansion will be different for each telescope since their fields of view are physically separated in the near field. It then becomes apparent that q and u possess harmonics of all orders viz.,

$$q = \cos(2\chi) - \frac{1}{2} \sum_{n=1}^{\infty} a_n \sin[(n+2)\chi] - b_n \cos[(n+2)\chi] - a_n \sin[(n-2)\chi] + b_n \cos[(n-2)\chi]$$

and

$$u = \sin(2\chi) + \frac{1}{2} \sum_{n=1}^{\infty} a_n \cos[(n+2)\chi] + b_n \sin[(n+2)\chi] + a_n \cos[(n-2)\chi] + b_n \sin[(n-2)\chi].$$

However, it is clear from examining the effects of standard instrumental imperfections such as, instrumental polarization, retardance in optical elements, cross-talk and scattering that odd harmonics can only come from the polarizer imperfections.

Also any zeroth order harmonics in measurements of q and u for a polarizer are also caused by polarizer imperfections since the instrumental polarization, at least to first order, only affects the $\sin 4\chi$ term. Thus a Fourier analysis of polarizer measurements is a powerful analysis tool, in the case where the polarizer zones are not perfectly aligned. Although terms in the Fourier expansion that have a $\sin 4\chi$ variation may be caused by instrumental polarization, they may also be caused by polarizer imperfections and there is no way of separating the two effects definitively. These terms should however be stable with respect to time if they are caused by instrumental polarization, whereas polarizer effects depend sensitively on the physical orientation of the polarizer sheet with respect to the RSP instrument and may therefore vary from one experiment to another. The fact that the $\sin 4\chi$ terms vary between experiments indicates that they may well be dominated by the effects of polarizer imperfections, while their magnitude can be regarded as an upper bound on instrumental polarization and is extremely small, generally less than 0.1%, as shown in table III below. The table shows the amplitude in percent polarization of the $\sin 4\chi$ variation in q and u , where the columns are from analyses of polarizer data acquired on different days. The columns marked i) are from 11-12-98, ii) from 11-20-98 and iii) from 02-22-99, while iv) is the average of the three values. The values in columns iv) are our current best estimate of the magnitude of instrumental polarization effects and given the effect of instrumental polarization shown in (2) it is apparent that for natural scenes (polarization less than 80%) we can neglect the effects of instrumental polarization the measured values of q and u .

Band	q (%)				u (%)			
	i)	ii)	iii)	iv)	i)	ii)	iii)	iv)
1	0.078	-0.064	-0.012	0.001	0.251	-0.070	-0.107	0.025
2	0.100	0.029	-0.025	0.035	-0.047	0.041	0.106	0.033
3	-0.084	-0.174	-0.063	-0.107	0.173	0.090	-0.010	0.084
4	0.101	0.007	-0.065	0.014	-0.042	0.061	0.127	0.049
5	-0.026	0.007	-0.078	-0.032	0.007	0.145	0.034	0.062
6	0.116	0.045	0.107	0.089	-0.172	0.068	-0.076	0.060
7	0.023	0.075	0.137	0.078	-0.019	0.018	-0.170	-0.057
9	0.049	0.189	0.150	0.129	-0.034	-0.034	-0.215	-0.094

Table III: Apparent instrumental polarization from Fourier analysis of polarizer data on three different days.

There are two other aspects of instrument performance/calibration that can be evaluated using the polarizer measurements. One is the degree to which scattering, straylight or cross talk is present. Since q and u should vary between ± 1 as the polarizers are rotated through 360° any observed reduction in the modulation depth below this amplitude can be ascribed to scattering and/or straylight and/or cross talk between the detectors in a given telescope. The observed modulation depth is typically 99.5%, or better and is the same for both telescopes in a given band (ie. q and u have the same modulation depth) to within 0.1%. The only band that does not conform to this behavior is the 2250nm channel where the modulation depth appears to be 97%. This low modulation depth may in fact be a result of the polarizers not generating a 100% polarized source at 2250nm, since HR polarizers start to exhibit degradation in their performance in this spectral region. This inconsistency compared with the behavior in the other channels is currently being investigated.

The final aspect of instrument performance that we evaluated using polarizer measurements was the relative orientation of the Wollaston prisms. These should be oriented so that the polarization axes are at 45° to one another. In this case $q = \cos 2\chi$ and $u = \sin 2\chi$ and a Fourier analysis should show that the variations of q and u , with 2χ periodicity, are in quadrature with respect to one another. In fact the prisms are not perfectly aligned, but by measuring the phase angle between q and u for the 2χ periodicity we can estimate the actual alignment of the Wollaston prisms. We can then correct the measurements of the degree and azimuth of polarization for this effect. Since the polarizers have variations in the orientation of their zones, as discussed above, we found that using measurements of a tilted glass plate provided a better estimate of the error in orientation of the Wollaston prisms, although the glass plate measurements and polarizer measurements do agree to within 0.1° .

The glass plate we used to estimate the alignment of the Wollaston prisms is a piece of Schott WG280 that is tilted to a fixed angle of 45° about an axis perpendicular to the line of sight. This glass plate was then rotated through 360° about the line of sight of the RSP instrument, with measurements being taken every 15° . A Fourier analysis was then performed to estimate the phase angle between the 2χ periodic variations of q and u . We found that the prism misalignments were consistent for all the bands in a given pair of telescopes, to within 1 arc minute, which demonstrates the high precision of the alignment of all the prisms within a given telescope assembly. The estimated relative error in orientation between the Wollaston prisms in telescopes 1 and 2 (q and u) was 0.435° for bands 1, 3 and 5, 0.245° for bands 2, 4 and 6 and 0.185° for bands 7, 8 and 9. As noted above, these errors in the alignment of the Wollaston prisms have no effect on the accuracy of the final measurement provided they are accurately known and can consequently be accurately corrected. We also used the glass plate as a source of weakly polarized light with a known state of polarization. The results are shown in figure 2 where calculated values of polarization at the different wavelengths are shown with a solid line, the dashed lines are for a glass plate

tilted to 44.8° and 45.2° and the measured values are shown by filled circles. There is extremely good agreement between the measured and calculated values with the maximum difference the two being 0.15% for the 2250nm band.

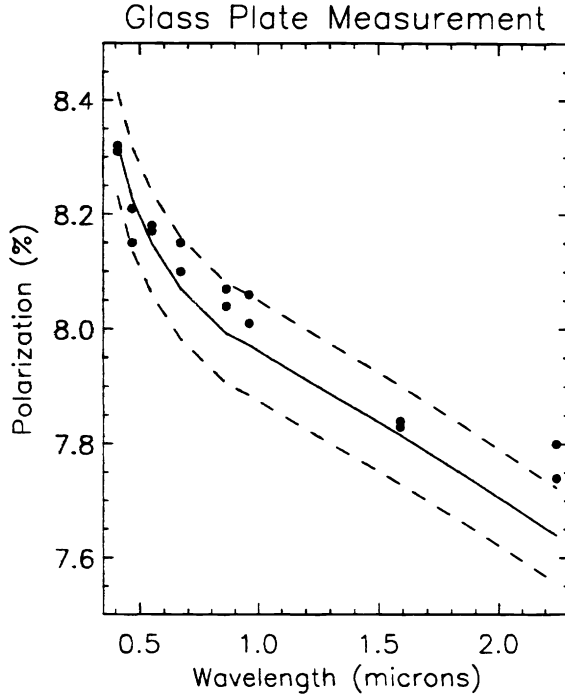


Figure 2: Comparison of calculated and measured polarization of a tilted glass plate.

2.1 Radiometric Calibration

A preliminary radiometric calibration of the RSP was performed on the top of La Cumbre Peak near Santa Barbara CA at an altitude of 990m (3250 feet) above a suppressed marine boundary layer. The radiometric calibration used a Spectralon reflectance standard illuminated by the sun at near normal incidence (11.6°). The RSP viewed the Spectralon over a range of angles of 47.2° to 67.2° with respect to the normal of the Spectralon and the Spectralon was oriented with its normal at 65° from the vertical in the solar principal plane. The model that was used for the radiance reflected by the Spectralon and measured by the RSP was that of a solar beam incident on an atmosphere containing an absorbing upper layer (ie. the stratosphere containing O₃ and NO₂) above a lower layer where Rayleigh and aerosol scattering takes place (ie. the troposphere). Since the Spectralon plate is tilted, the appropriate weighted integration of the diffuse downwelling radiance needs to be performed. In the equation given below and in determining the calibration coefficients for the RSP the exact convolution between the downwelling radiation and the BRDF of the tilted Spectralon plate is not used. Instead the irradiance illuminating the tilted plate is calculated and it is then assumed that this irradiance is scattered with a Lambertian distribution with the magnitude of the reflection being given by the Spectralon albedo \bar{R}_{spec} . This provides a reasonable approximation for the reflection of *diffuse* illumination by the Spectralon plate. The intensity observed by the RSP is therefore given by the expression

$$I(\mu) = \frac{F_0 \exp(-\tau_{str} / \mu_0)}{\pi R^2} c(\mu)$$

where

$$c(\mu) = \left[\mu_{AOI} R_{spec}(\mu, \mu_{AOI}; 0) \exp(-\tau_{trop} / \mu_0) + \mu_0 \bar{R}_{spec} \int_{n \cdot s' > 0} D(\mu', \mu_0; \phi') n \cdot s' d\mu' d\phi' \right]$$

μ_{AOI} is the cosine of the angle of incidence of the direct solar beam on the Spectralon plate, μ is the cosine of the angle between the RSP viewing direction and the normal to the Spectralon plate, μ_0 is the cosine of the solar zenith angle, ϕ' is the azimuth with respect to the sun. F_0 is the solar flux at the top of the atmosphere when the sun is 1 A.U. from the earth, R is the sun-earth distance in A.U., $R_{spec}(\mu, \mu_{AOI}; 0)$ is the BRDF of the Spectralon^{1,2}, τ_{strat} is the extinction optical depth of the absorbing gases O₃ and NO₂, τ_{trop} is the extinction optical depth of aerosol and Rayleigh scatterers, $D(\mu', \mu_0; \phi')$ is the

distribution of downwelling radiation, \mathbf{n} is the unit normal of the Spectralon plate and \mathbf{s}' is the unit vector associated with the direction of the radiation hitting the Spectralon plate.

For the interpretation of the data from the RSP a radiance based calibration coefficient is not necessary since we will always be looking at scattered solar radiation. We therefore calibrate the instrument so that the expression for the intensity given in (1) is actually a normalized radiance $i(\mu) = \pi I(\mu)/F_0$ which leads to the following expression for the radiometric calibration coefficient A

$$A = \frac{[S1L(spectralon) + K1 \times S1R(spectralon)] \times R^2}{\exp(-\tau_{str}/\mu_0) \times c(\mu)}$$

The optical depths for O_3 and NO_2 are based on climatological values for the column burden of each gas multiplied by an extinction coefficient. The extinction coefficients are based on a solar spectrum weighted integration of the cross-sections for each gas over the spectral bandpass of each channel. The Rayleigh optical depth is based on the formula given by Hansen and Travis³ corrected for altitude and the aerosol optical depth is estimated from the sky polarization measurements⁴ that are presented in section 3. If the function $c(\mu)$ is being evaluated correctly, and in particular if the Spectralon BRDF^{1,2} is correct, the value of A should be invariant with respect to the angle that the RSP views the Spectralon plate. In figure 3 shown below the dashed lines are the estimated values of A for all the channels except the 1880nm channel, while the solid lines are the average values of A over the center of the Spectralon plate.

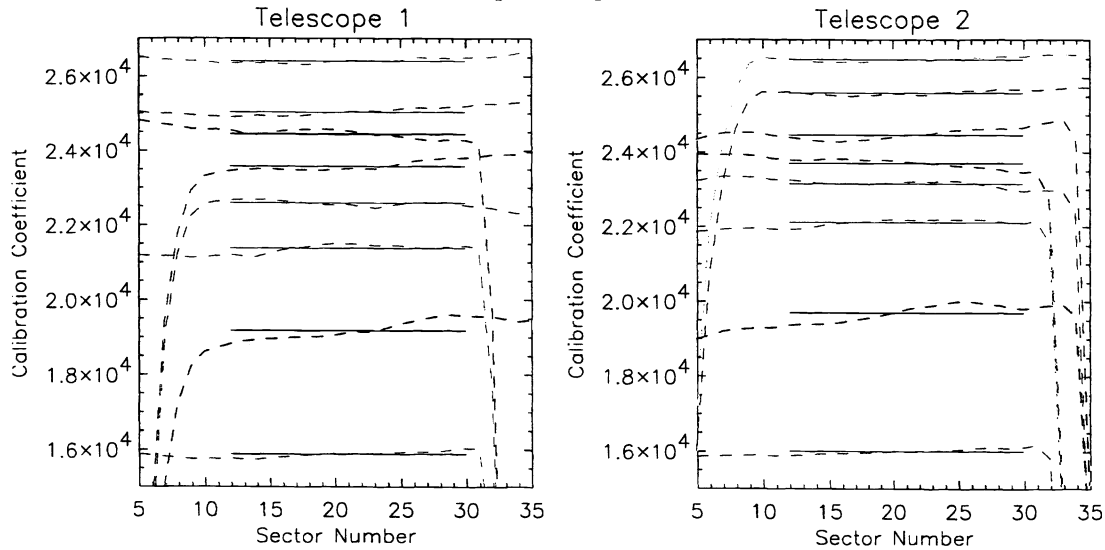


Figure 3: Check of angular consistency between RSP measurements and BRDF data from other Spectralon plates.

While most of the measurements of A are quite flat, indicating good consistency between the theoretical and actual $c(\mu)$ functions, it is apparent that the second and third dashed lines from the bottom of each figure, that correspond to the 410nm and 470nm bands respectively, show significant variation of calibration coefficient A as a function of view angle (sector number). Given the nature of the available Spectralon BRDF data it is not clear why this is the case and so the radiometric calibration of these channels must be regarded as more uncertain than the other channels. We are currently examining whether an exact integration of the Spectralon BRDF with the downwelling sky radiation is required for these bands, in which the diffuse contribution to the spectral illumination is quite large. However the accuracy with which this can be done is limited by the absence of BRDF data for the Spectralon plate we are using, or tabulated data for similar plates at the wavelengths of interest.

3. MEASUREMENTS

3.1 Upward looking measurements

As an example of the type of information that can be derived from polarimetry, we show below upward looking measurements of the sky polarization and radiance in the 410, 470, 555, 670 and 865nm bands. The observations are shown with their error bars (0.3% for polarization and 5% for radiance). A simple look up table of atmospheric models with different aerosol effective radii, refractive indices, optical depths and different surface albedoes was searched to find a best fit to the data. The model found from this look up table was then used as the starting point for a Newton-Raphson iterative search

for the aerosol model that best fits the observations. This model fit is shown with a dashed line and is almost indistinguishable from the observations (0.3% RMS deviation).

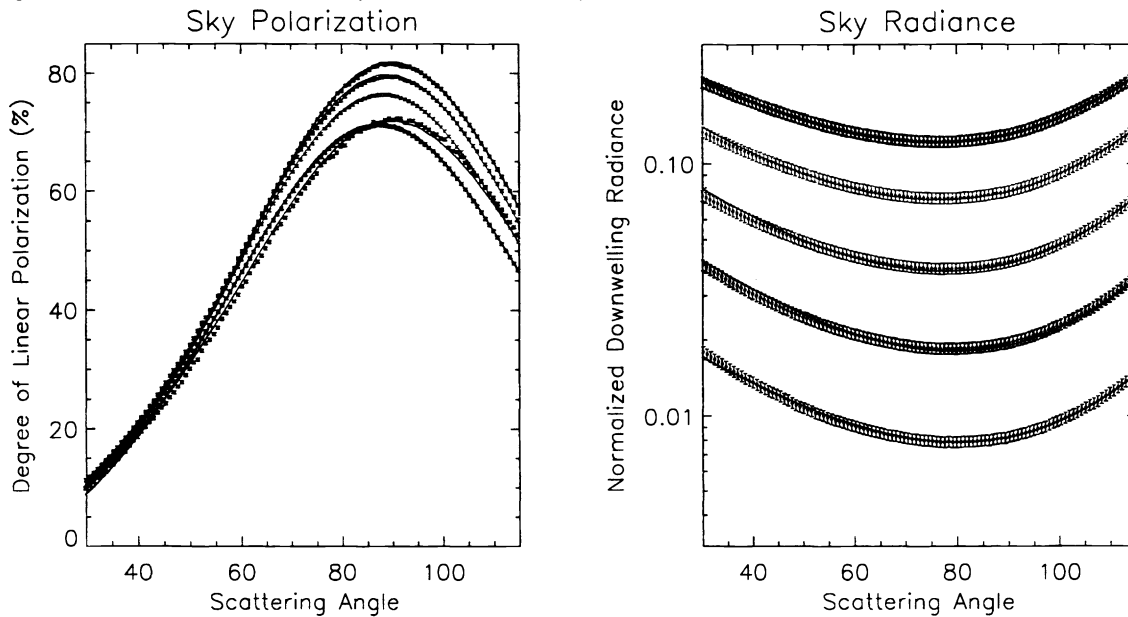


Figure 4: Upward looking sky radiance measurements taken on a mountain top.

The intensity measurements were not used in the estimation of the aerosol model and can therefore be regarded as a partially independent check of the radiometric calibration. The root mean square relative deviation between the measured and modelled intensity is 3%, which is the expected radiometric calibration uncertainty for this instrument. The aerosol model that was found to be the best fit to the polarization data had an effective radius of $0.12\mu\text{m}$, a refractive index of 1.38 and an optical depth of 0.01. These measurements were made at 990m (3250ft.) above sea level near Santa Barbara CA, well above the marine boundary layer.

As an example of the method when the data is not almost pure Rayleigh scattering we show a similar figure for measurements at sea level. These measurement were taken on a day when there were forest fires in Southern California, so the aerosol loading is partially smoke, although this was not apparent visually.

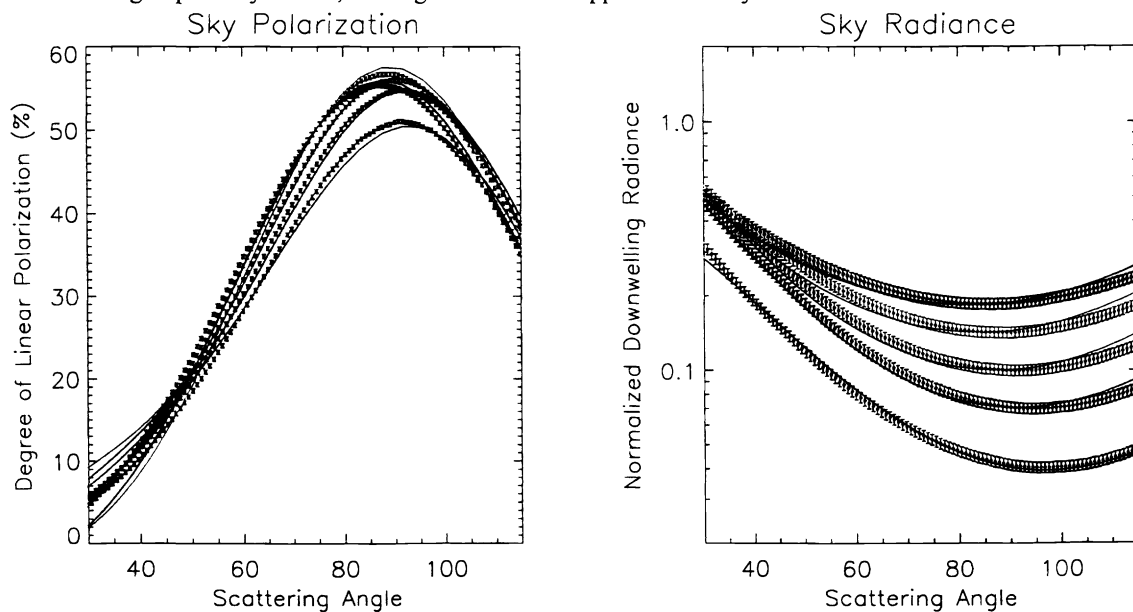


Figure 5: Upward looking sky radiance measurements taken at sea level with smoke aerosols present.

The aerosol model that was found to be the best fit to the polarization data had an effective radius of $0.2\mu\text{m}$, a refractive index of 1.5 and an optical depth of 0.125. This refractive index is consistent with polarimetric nephelometer measurements of smoke aerosols³. No attempt has been made so far to fit the data to a multimodal aerosol distribution, though this is feasible and has been demonstrated on simulated data sets⁴.

3.2 Downward looking measurements

The RSP instrument has recently been used to take downward looking measurements from a light aircraft. The figures below show measurements made by the RSP at 670nm and 865nm over the ocean near Santa Barbara CA. The right side of each figure is dominated by sunglint which limits the angular range that is sensitive to aerosol scattering. The dots in each figure are the measurements, while the solid lines are an aerosol model calculation with an optical depth of 0.1, a refractive index of 1.36 and an effective radius of 0.7 microns. This model was found to be the best fit using a table look up approach with relatively coarse resolution of the retrieved parameters and only allowing the effective radius of the size distribution to vary. The dashed lines represent an aerosol model with an optical depth of 0.1, a refractive index of 1.5 and an effective radius of 0.7 microns. This shows what effect choosing the wrong refractive index can have. Evidently if only intensity measurements were available and the refractive index was prescribed to be 1.5 the retrieved optical depth and size distribution would be incorrect.

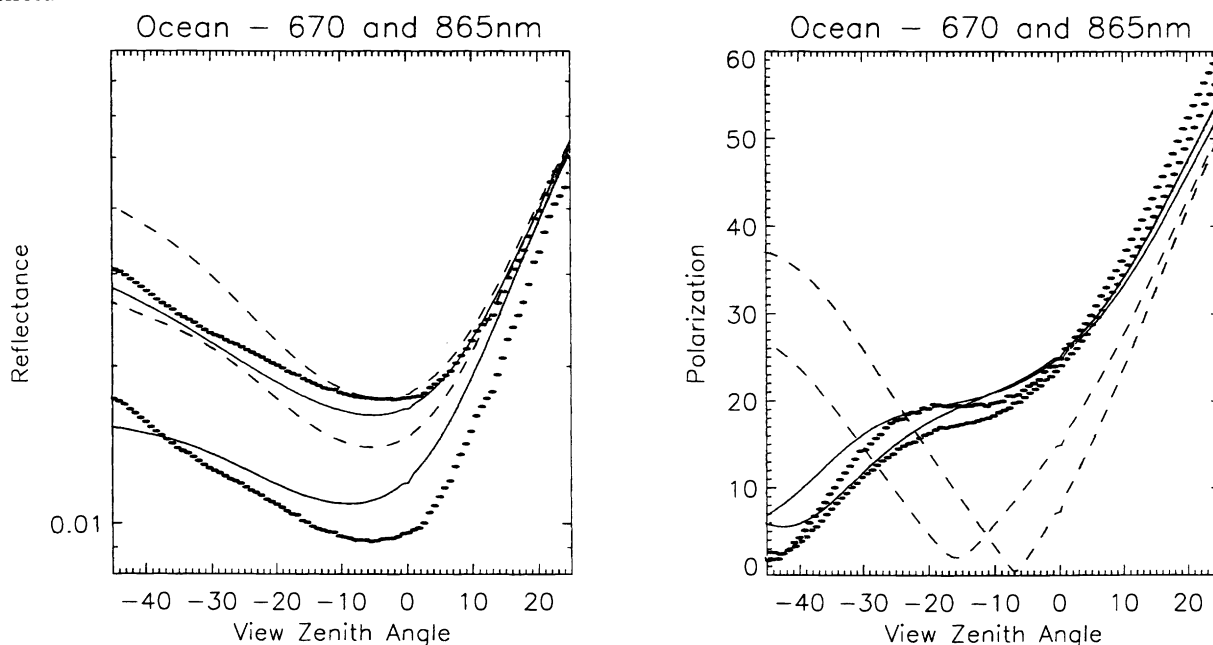


Figure 6: Aircraft observations taken over the Pacific ocean near the solar principal plane.

4. CONCLUSIONS

The RSP instrument has been polarimetrically and radiometrically calibrated. The results of these calibration efforts indicate that instrumental polarization effects are less than 0.1%, while the relative gains of pairs of detectors for a given band are stable to within 0.1% over the course of a day for all channels other than telescope 1 of band 7 which exhibits a somewhat larger drift. The results of ground-based and aircraft-based measurements have been analysed and have been found to be consistent with our understanding of the polarization of scattered sunlight. The retrieval of aerosol radiative properties from such data is fairly straightforward and provides strong constraints on aerosol size distributions and refractive indices. The analysis of the data presented here will be described in greater detail in a forthcoming publication.

5. FUTURE EFFORTS

We hope to validate the RSP's instrumental measurements against the more widely used and understood measurements of sunphotometers and sky radiometers in the coming months. This effort is designed to test whether the

theoretical expectations about the accuracy of aerosol optical depth retrievals using polarization measurements are consistent with other observations. We will also be analysing aircraft data taken over land surfaces and large lakes to test algorithms for aerosol retrievals over land.

6. ACKNOWLEDGEMENTS

The Research Scanning Polarimeter was fabricated at SpecTIR Corporation evolved from a collaborative effort among many contributors. Key design elements were provided by Richard Chandos (electronics), Roland Davis (mechanics) and Edgar Russell (systems/optics). The data used in this paper were purchased from SpecTIR under an award from NASA's EOS program.

7. REFERENCES

1. J. C. Fleming, Ultraviolet BRDF of selected materials, *Proc. SPIE*, **2864**, pp.406-415, 1996.
2. B.T. McGuckin, D.A. Haner and R.T. Menzies, Multiangle Imaging Spectroradiometer: optical characterization of the calibration panels, *Appl. Opt.*, **36**, pp.7016-7022, 1997.
3. J.E. Hansen and L.D. Travis, Light scattering in planetary atmospheres, *Space Sci. Rev.*, **16**, pp.527-610, 1974.
4. B. Cairns, B.E. Carlson, A.A. Lacis and E.E. Russell, An analysis of ground-based polarimetric sky radiance measurements, *Proc. SPIE*, **3121**, 383-393, 1997.
5. V.V. Veretennikov, V.S. Kozlov, I.E. Naats and V.Ya. Fadeyev, On the determination of the optical constants and microstructure of smoke aerosols from optical polarization measurements. *Izv. Atmos. Oceanic Phys.*, **16**, 177-181, 1980.